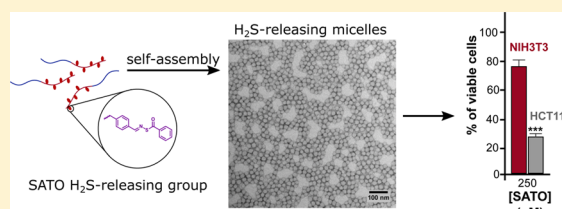


H₂S-Releasing Polymer Micelles for Studying Selective Cell Toxicity

Jeffrey C. Foster,[†] Scott C. Radzinski,[†] Xianlin Zou,[‡] Carla V. Finkielstein,[‡] and John B. Matson^{*,†}[†]Department of Chemistry, Macromolecules Innovation Institute, and Center for Drug Discovery, Virginia Tech, Blacksburg, Virginia 24061, United States[‡]Department of Biological Sciences and Biocomplexity Institute, Virginia Tech, Blacksburg, Virginia 24061, United States

S Supporting Information

ABSTRACT: We report the preparation of *S*-aroylthiooxime (SATO) functionalized amphiphilic block copolymer micelles that release hydrogen sulfide (H₂S), a gaseous signaling molecule of relevance to various physiological and pathological conditions. The micelles release H₂S in response to cysteine with a half-life of 3.3 h, which is substantially slower than a related small molecule SATO. Exogenous administration of H₂S impacts growth and proliferation of cancer cells; however, the limited control over H₂S generation from inorganic sulfide sources results in conflicting reports. Therefore, we compare the cellular cytotoxicity of SATO-functionalized micelles, which release H₂S in a sustained manner, to Na₂S, which releases H₂S in a single dose. Our results show that H₂S-releasing micelles significantly reduce the survival of HCT116 colon cancer cells relative to Na₂S, GYY4137, and a small molecule SATO, indicating that release kinetics may play an important role in determining toxicity of H₂S toward cancer cells. Furthermore, H₂S-releasing micelles are well tolerated by immortalized fibroblasts (NIH/3T3 cells), suggesting a selective toxicity of H₂S toward cancer cells.



KEYWORDS: gasotransmitter, H₂S donors, controlled release, polymer amphiphiles, RAFT

INTRODUCTION

Hydrogen sulfide (H₂S) belongs to a classification of biologically relevant signaling gases known as gasotransmitters.¹ Gasotransmitters, which also include nitric oxide (NO) and carbon monoxide (CO), have attracted much interest in recent years due to their extensive roles in cellular signaling.² For example, H₂S regulates vasodilation, promotes angiogenesis, and generally exhibits beneficial effects as an anti-inflammatory agent.^{3–8} To support these biological studies, new chemical tools have been developed over the past ~5 years. These include H₂S sensors, which report on H₂S concentrations in vivo and in vitro,^{9–12} compounds triggered by endogenous H₂S to release drugs,¹³ and compounds that release H₂S (H₂S donors),^{14–22} usually through decomposition reactions initiated by a specific trigger.

The gaseous nature of H₂S and its fast reactivity in biological systems make controlled delivery a necessity and a difficult challenge. To date, most studies of H₂S biology have been conducted with sulfide salts (Na₂S and NaSH). These inorganic sulfide sources generate H₂S instantaneously upon dissolution, resulting in a rapid surge in H₂S concentration followed by a rapid decline. While experimentally convenient, sulfide salts can convolute the results of biological studies due to their rapid release, as the activity of H₂S profoundly depends on its local concentration. For example, evidence suggests that H₂S could be an effective therapeutic candidate due to its ability to selectively reduce survival in cancer cells.^{23,24} This is likely the result of the high set point of oxidative stress that cancer cells maintain, making them more susceptible than healthy cells to the

cytotoxic pro-oxidant effects exhibited by H₂S in highly oxidative environments.²⁵ Additionally, H₂S passes through biological membranes without active transport mechanisms,³ which may enable deep penetration into the tumor interstitium, a major problem with traditional small molecule chemotherapeutics.²⁶ Conversely, endogenous levels of H₂S provide a route for some cancer cells to evade standard treatment strategies by promoting angiogenesis, augmenting mitochondrial bioenergetics, activating antiapoptotic pathways, and controlling cell cycle progression.^{27,28} This apparent discrepancy over the response of cancer cells to H₂S may arise from different release rates among different H₂S donors.²³ Therefore, this and other challenges in H₂S biology may be resolved by developing advanced delivery vehicles that produce well-defined quantities of H₂S over controllable time scales.

In the past few years, reports have appeared of a multitude of H₂S-releasing small molecules that more aptly mimic the sustained endogenous production of the gas in vivo.^{14–22} However, many small molecule H₂S donors suffer from limitations such as ill-defined release mechanisms, poor water solubility, and inherent (or latent) toxicity. Such small molecule H₂S donors also typically have no capacity for targeting any specific organ and therefore only provide systemic delivery of H₂S. More recently, a handful of polymers that release H₂S

Received: December 13, 2016

Revised: February 14, 2017

Accepted: February 28, 2017

have addressed some shortcomings of small molecule H₂S donors.^{29–33} However, these also have limitations: linear polymers are typically too small to avoid rapid renal clearance in the bloodstream and have limited capacity for targeting a specific site in the body. Polymer micelles made from amphiphilic block copolymers address these challenges because they are typically in the ideal size range (20–100 nm) for long bloodstream circulation and can target specific sites in the body (e.g., a solid tumor) through either passive or active mechanisms.^{34,35} Polymer micelles that combine controlled H₂S release with the capacity for in vivo targeting and long bloodstream circulation are therefore needed to advance the field of H₂S biology and to develop novel therapeutics. We present in this report initial efforts to develop polymer micelles as advanced H₂S delivery vehicles, which we use here for studying toxicity toward a cancer cell line.

MATERIALS AND METHODS

Materials. All reagents were obtained from commercial vendors and used as received unless otherwise stated. 2,2'-Azobis(2-methylpropionitrile) (AIBN) was recrystallized from methanol prior to use. S-Aroylthiohydroxylamine (SATHA) and SATO1 ((C₆H₅)C=OSN=CH(C₆H₄)COOH) were prepared according to a previously reported procedure.¹⁷ The monomer 2-(4-formylbenzoyloxy)ethyl methacrylate (FBEMA) was also synthesized as previously reported.²⁹ Dry solvents were purified by passage through a solvent purification system (MBraun).

Methods. NMR spectra were measured on an Agilent 400 MHz spectrometer. ¹H and ¹³C NMR chemical shifts are reported in ppm relative to internal solvent resonances. Yields refer to chromatographically and spectroscopically pure compounds unless otherwise stated. Size exclusion chromatography (SEC) was carried out in THF at 1 mL/min at 30 °C on two Agilent PLgel 10 μm MIXED-B columns connected in series with a Wyatt Dawn Heleos 2 light scattering detector and a Wyatt Optilab Rex refractive index detector. No calibration standards were used, and dn/dc values were obtained by assuming 100% mass elution from the columns. TEM samples were drop cast from 1 mg/mL solutions of micelles in H₂O onto carbon-coated copper 300 mesh TEM grids (Electron Microscopy Sciences). Samples were then stained with a 2% solution of uranyl acetate in water. Images were taken on a Philips EM420 TEM with a slow scan CCD camera. UV–vis absorbance spectra were recorded on a Cary 5000 UV–vis spectrophotometer (Agilent) from 800 to 550 nm or on a Spectramax M2 plate reader (Molecular Devices). Dynamic light scattering (DLS) was conducted using a Malvern Zetasizer Nano operating at 25 °C. A solution of micelles was prepared at 1 mg/mL and filtered with a 0.2 μm filter prior to scanning. The calculations of the particle size distributions and distribution averages were conducted using CONTIN particle size distribution analysis routines with intensity averages. Measurements were made in triplicate, and errors reflect standard deviations.

Synthesis of 4-Cyano-4-(dodecylsulfanylthio-carbonyl)sulfanyl Pentanoic Acid (CTA). Dodecanethiol (10 mL, 41.7 mmol) was dissolved in hexanes (150 mL) in a round-bottom flask. To the flask was added a solution of potassium *tert*-butoxide (4.68 g, 41.7 mmol) in THF (50 mL). The reaction mixture was stirred at rt for 20 min. CS₂ was added (2.7 mL, 44.7 mmol), and the reaction mixture was stirred for an additional 1 h. I₂ was then added in portions until

the reaction mixture maintained a persistent dark brown color. The reaction mixture was stirred overnight at rt. The reaction mixture was transferred to a separatory funnel and washed consecutively with 10% Na₂S₂O₃, H₂O, and brine. The organic layer was then dried over Na₂SO₄ and rotovapped.

The resulting viscous yellow oil (22.8 g, 41.1 mmol) was redissolved in EtOAc (100 mL) in a round-bottom flask. To the flask was added 4,4'-azobis(4-cyanovaleric acid) (11.6 g, 41.4 mmol). The reaction mixture was heated at reflux overnight. Silica gel was poured into the reaction flask, and the silica slurry was rotovapped to dryness. The silica was then dry-loaded onto a silica gel column, eluting with 9:1 hexanes/EtOAc. The product-containing fractions (*R*_f ≈ 0.3 in the mobile phase) were combined and rotovapped to give the product as a yellow solid (9.50 g, 57% yield). ¹H NMR (CDCl₃): δ 3.33 (t, *J* = 4 Hz, 2H), 2.68 (t, *J* = 4 Hz, 2H), 2.54 (m, 1H), 2.39 (m, 1H), 1.88 (s, 3H), 1.69 (q, *J* = 8 Hz, 2H), 1.45–1.19 (m, 18H), 0.88 (t, *J* = 4 Hz, 3H). ¹³C NMR (CDCl₃): δ 216.88, 177.63, 118.99, 46.30, 37.21, 33.58, 32.03, 29.74, 29.67, 29.66, 29.54, 29.46, 29.19, 29.05, 27.78, 24.96, 22.81, 14.25. HR-MS: [M + H]⁺ calculated 404.1746; found 404.1749.

Synthesis of macroCTA. A round-bottom flask was charged with CTA (0.81 g, 2.01 mmol), polyethylene glycol monomethyl ether (*M*_n = 5000 g/mol, 2.0 g, 0.400 mmol), 4-dimethylamino pyridine (0.12 g, 0.982 mmol), and anhydrous CH₂Cl₂ (40 mL). *N,N'*-Dicyclohexylcarbodiimide (DCC) (0.41 g, 1.99 mmol) was dissolved in 5 mL of anhydrous CH₂Cl₂ in a vial. The DCC solution was added dropwise to the flask containing the other reagents, and the reaction mixture was stirred at rt overnight. The precipitated solids were removed by filtration. The desired product was isolated via precipitation from diethyl ether and was purified by repeated precipitations (2–4) from CH₂Cl₂ into diethyl ether to afford the product as a yellow solid (1.50 g, 69% yield). ¹H NMR (CDCl₃): δ 4.24 (t, *J* = 4 Hz, 2H), 3.80 (t, *J* = 4 Hz, 2H), 3.71–3.51 (m, 494H), 3.45 (t, *J* = 4 Hz, 2H), 3.36 (s, 3H), 3.31 (t, *J* = 8 Hz, 2H), 2.64 (t, *J* = 8 Hz, 2H), 2.51 (m, 1H), 2.37 (m, 1H), 1.86 (s, 3H), 1.68 (t, *J* = 8 Hz, 2H), 1.42–1.18 (m, 18H), 0.87 (t, *J* = 4 Hz, 3H).

Synthesis of PEG-*b*-poly(FBEMA). A typical polymerization procedure is as follows: To an oven-dried Schlenk tube equipped with a magnetic stir bar was added macroCTA (127 mg, 25.0 μmol), FBEMA (1.00 g, 3.81 mmol), and 5 mL of anhydrous DMF. A solution of 2,2'-azobis(2-methylpropionitrile) (AIBN) was prepared by dissolving 4.2 mg (2.54 μmol) in 1 mL of anhydrous DMF in a vial. One hundred microliters of this solution was added to the Schlenk tube. The tube was deoxygenated by subjecting the contents to three freeze–pump–thaw cycles. The Schlenk tube was then backfilled with N₂ and submerged in an oil bath maintained at 75 °C. Samples were removed periodically by N₂-purged syringe to monitor molecular weight evolution by SEC and conversion by ¹H NMR spectroscopy. The polymerization was quenched by submerging the tube into liquid N₂ and exposing the reaction solution to air. The resulting PEG-*b*-poly(FBEMA) was isolated via precipitation from diethyl ether. If necessary, further precipitations from CH₂Cl₂ into diethyl ether were performed to remove residual monomer.

Removal of Dithioester End Group. A round-bottom flask was charged with PEG-*b*-poly(FBEMA) (0.50 g, 14.0 μmol), AIBN (47.0 mg, 284 μmol), and 1,4-dioxane (3 mL). The flask was outfitted with a condenser, and the reaction mixture was heated in an oil bath maintained at 80 °C for 1.5 h.

The reaction mixture was allowed to cool to rt, and the polymer was recovered via precipitation into diethyl ether.

Addition of SATHA to PEG-*b*-poly(FBEMA). A general procedure for the SATO formation reaction is as follows. Following end group removal, PEG-*b*-poly(FBEMA) (100 mg, 3.21 μmol) was dissolved in CH_2Cl_2 (3 mL) in a 1 dram vial. To the vial was added SATHA (147 mg, 962 μmol) in one portion. Approximately 10 μL of trifluoroacetic acid (TFA) was added as a catalyst. The reaction mixture was left to stand at rt for 16 h over molecular sieves. ^1H NMR spectroscopy was conducted after this time to determine the conversion of aldehyde to SATO. The modified polymer was recovered via precipitation into diethyl ether.

Determination of Critical Micelle Concentrations (CMCs). A micelle stock solution was prepared at 0.1 mg/mL in H_2O . This solution was diluted with water to afford concentrations of 0.05, 0.04, 0.03, 0.02, 0.01, 0.005, 0.001, 0.0001, 0.00001, and 0.000001 mg/mL. Two microliters of a 1 mg/mL Nile red solution in acetone was added to each dilution to make a final volume of 2 mL. The samples were transferred to a 96-well plate and were placed in a vacuum oven set to 30 $^\circ\text{C}$ for at least 2 h to ensure complete evaporation of acetone. Fluorescence emission spectra were recorded for each sample ($\lambda_{\text{ex}} = 530 \text{ nm}$), and the emission intensity at 630 nm was plotted against $\log(\text{concentration})$. The CMC value was taken to be the intersection between the linear fits of the high and low concentration regimes.

H_2S Release Kinetics via the Methylene Blue Method. Reactions for kinetics studies were run in triplicate, with each reaction vial containing 20 μL of phosphate buffer (1 M in H_2O , pH = 7), micelle solution (volume dependent on polymer concentration and SATO loading), 100 μL of $\text{Zn}(\text{OAc})_2$ solution (40 mM in H_2O), 20 μL of cysteine solution (100 mM in H_2O), and DI H_2O to make 2 mL total volume. Final concentrations were 250 μM SATO functional groups, 2 mM $\text{Zn}(\text{OAc})_2$, and 1 mM Cys. A blank solution was also run for each experiment that did not contain micelles. At predetermined time points, 100 μL was removed from each vial. Each 100 μL aliquot was diluted with 100 μL of FeCl_3 solution (30 mM in 1.2 M HCl) followed by 100 μL of *N,N*-dimethyl-*p*-phenylenediamine (20 mM in 7.2 M HCl). Aliquots were stored for a minimum of 24 h after the final aliquot had been taken. The absorbance of each sample was measured at 750 nm using a plate reader. Kinetic analysis was done by subtracting the absorbance of the blank solution from the average absorbance at each time point. First-order half-lives of H_2S release were determined by plotting time vs $\ln(1/(1 - \% \text{ released}))$, with $t_{1/2} = \ln(2)/\text{slope}$. The conversion of the reaction was obtained by normalizing the absorbance values to the maximum absorbance that was measured for each experiment (or the value at which the plot of absorbance vs time reached a plateau).

Calibration Procedure for the Methylene Blue Assay. A 15 mM Na_2S stock solution was prepared by dissolving 24 mg of Na_2S in 20 mL of DI H_2O . This solution was then diluted 10 \times with H_2O to give a 1.5 mM Na_2S solution. Na_2S solutions at concentrations ranging from 5 to 100 μM were prepared in triplicate by mixing the appropriate volume of 1.5 mM Na_2S stock solution with 20 μL of 1 M phosphate buffer and then diluting with DI H_2O to a total volume of 1 mL. Samples were prepared by removing 100 μL of each Na_2S solution and diluting with 100 μL of FeCl_3 solution (30 mM in 1.2 M HCl) followed by 100 μL of *N,N*-dimethyl-*p*-phenyl-

enediamine (20 mM in 7.2 M HCl). Aliquots were stored for a minimum of 24 h after the final aliquot had been taken. The absorbance of each sample was measured at 750 nm using a plate reader. A calibration curve was prepared by plotting absorbance for each data point as a function of $[\text{Na}_2\text{S}]$.

H_2S Release Profile via the Methylene Blue Method. Reactions for measurement of the H_2S release profile were conducted in triplicate, with each reaction vial containing 20 μL of phosphate buffer (1 M in H_2O , pH = 7), micelle solution (volume dependent on polymer concentration and SATO loading), 20 μL of cysteine solution (100 mM in H_2O), and DI H_2O to make 2 mL total volume. Final concentrations were 250 μM SATO functional groups and 1 mM Cys. A blank solution was also run for each experiment that did not contain micelles. Additional controls without Cys were also conducted with and without micelles. At predetermined time points, 100 μL was removed from each vial. Each 100 μL aliquot was diluted with 100 μL FeCl_3 solution (30 mM in 1.2 M HCl) followed by 100 μL of *N,N*-dimethyl-*p*-phenylenediamine (20 mM in 7.2 M HCl). Aliquots were stored for a minimum of 24 h after the final aliquot had been taken. The absorbance of each sample was measured at 750 nm using a plate reader. The concentration of H_2S at each time point was then plotted using the calibration curve.

Cell Culture and Clonogenic Survival Assay. Colorectal carcinoma HCT116 cells (ATCC CCL-247) and embryonic fibroblast NIH/3T3 cells (ATCC CRL-1658) were obtained from ATCC. HCT116 cells were propagated in HyClone McCoy's 5a medium (GE Healthcare), supplemented with 10% fetal bovine serum (Corning), 50 IU/mL penicillin, and 50 $\mu\text{g}/\text{mL}$ streptomycin (MP Biomedicals). Fibroblasts were maintained in ATCC-formulated Dulbecco's modified Eagle's medium supplemented containing 10% calf serum (ATCC 31334) and penicillin/streptomycin antibiotics as above. For all experiments, cells were maintained at 37 $^\circ\text{C}/5\% \text{ CO}_2$ until reaching 50–80% confluence.

For clonogenic assays, exponentially growing HCT116 or NIH/3T3 cells were harvested, and various dilutions of cells (500 to 2000 cells/well) were seeded into 6-well plates and allowed to attach overnight in the incubator before adding different formulations. Each cell type was titrated with various dose-concentration of SATO groups in active micelles ranging from 50 to 250 μM in the presence of 1 mM Cys for ~ 6 h. Corresponding controls include cells treated with 50–250 μM Na_2S , active micelles at 250 μM SATO in the absence of Cys, inactive micelles lacking the SATO group (250 μM aldehyde precursor) in the presence or absence of 1 mM Cys, or 1 mM Cys alone. Plates were transferred to 37 $^\circ\text{C}/5\% \text{ CO}_2$ until cells in control wells had formed sufficiently large clones (~ 10 days), after which they were fixed with a mixture of 6% glutaraldehyde/0.5% crystal violet for 30 min at room temperature. After removing the fixative, plates with colonies were allowed to dry at room temperature before manual counting. The surviving fraction of cells after treatment was calculated, taking into account the plating efficiency of control cells. All experiments were performed in triplicate, and the means and standard deviations were plotted using Excel and tested for statistical significance using a paired *t* test.

RESULTS AND DISCUSSION

We recently reported on the *S*-aroylthiooxime (SATO) functional group, which represents one type of versatile H_2S donor.¹⁷ SATOs were efficiently prepared in one step via

reaction of an *S*-aroylthiohydroxylamine (SATHA) with an aromatic aldehyde. H₂S release from SATOs was selectively triggered by a thiol, and release kinetics were fine-tuned by manipulating the substituents on the aromatic ring of the parent *S*-aroylthiohydroxylamine, with half-lives of release ranging from 8–82 min under the conditions tested. The SATO-forming reaction was also recently used for postpolymerization modification to prepare H₂S-releasing polymers.²⁹ Based on the versatility and robustness of SATOs, we sought to prepare a new type of supramolecular H₂S donor that exhibited sustained release, would possess enhanced pharmacokinetics *in vivo*, and could be further functionalized for specific tissue targeting to solid tumors.

To prepare a SATO-containing polymer amphiphile, a PEGylated chain transfer agent (CTA) for reversible addition–fragmentation chain transfer (RAFT) polymerization was synthesized. This macroCTA was employed in RAFT polymerization of 2-(4-formylbenzoyloxy)ethyl methacrylate (FBEMA) in the presence of 2,2'-azobis(2-methylpropionitrile) (AIBN) to produce a block copolymer of the form PEG-*b*-poly(FBEMA) (Figure 1A). The block polymer was of narrow

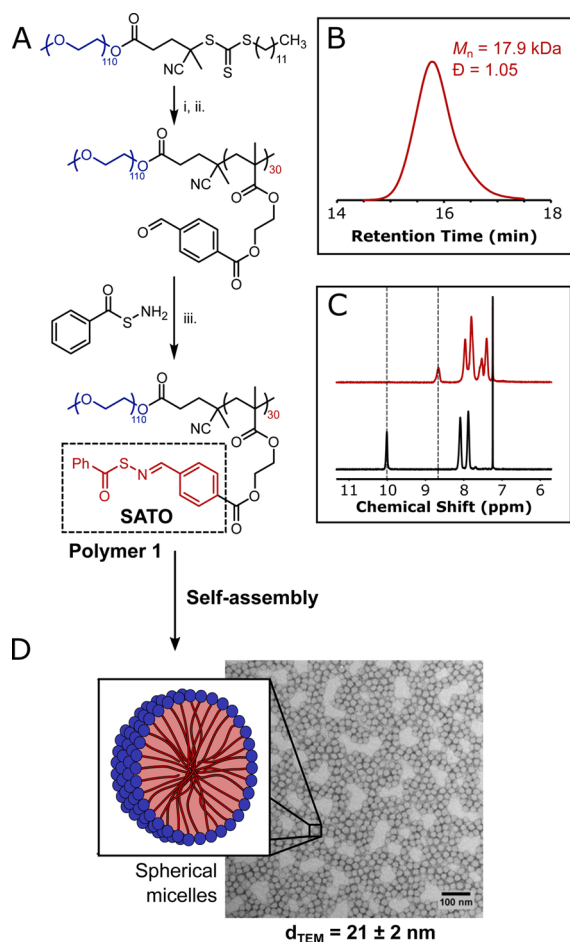


Figure 1. Synthesis of SATO-containing polymer 1. (A) Synthetic route. Experimental conditions: (i) FBEMA, AIBN, DMF, 70 °C; (ii) AIBN, dioxane, reflux; (iii) CH₂Cl₂, molecular sieves, TFA (cat), rt. (B) SEC trace of polymer 1. (C) ¹H NMR spectrum before (bottom trace) and after (top trace) SATO formation. Dashed lines at 10.0 and 8.6 ppm highlight the aldehyde and SATO resonances, respectively. (D) Conventional TEM image and schematic illustration of self-assembled micelles of polymer 1.

dispersity ($\bar{D} = 1.05$) with a monomodal molecular weight distribution (Figures 1B and S8). A high degree of chain end functionalization with the desired PEG block was confirmed by comparing polymer number-average molecular weights (M_n s) measured by SEC (13.8 kDa), calculated from monomer conversions (13.5 kDa), and determined by ¹H NMR end group analysis (13.2 kDa).

The thiocarbonyl-thio moiety can react with nucleophiles such as thiols to yield a variety of sulfur-containing byproducts, including H₂S.³⁶ Therefore, the trithiocarbonate end groups at the ω -chain ends were displaced by using an excess of AIBN in refluxing dioxane (Figures 1A and S12), as reported previously.²⁹ The polymer was then treated with 2 equiv of *S*-benzoylthiohydroxylamine in the presence of catalytic trifluoroacetic acid (TFA) to afford block copolymer 1. ¹H NMR spectroscopy confirmed complete SATO formation. Importantly, SATO formation did not increase the modality of the SEC trace (Figure S8); the expected increase in molecular weight was observed (from 13.8 kDa to 17.9 kDa) in accordance with the added mass of the newly formed SATOs (Table S1).

To prepare H₂S-releasing micelles, the block copolymers were dissolved in THF, diluted with an equal volume of H₂O, and dialyzed against H₂O for 48 h. TEM revealed uniform spherical particles of average diameter of 21 ± 2 nm (Figures 1D and S12). This diameter represents the dimension of the hydrophobic micelle core, as the hydrophilic PEG coronae are not typically observed via TEM. The observed core diameter matches the expected value for spherical micelles of ~19 nm calculated assuming fully extended SATO block chains. DLS further confirmed a single population of aggregates of diameter 38 ± 4 nm (Figure S9). The slightly smaller size obtained from TEM is unsurprising as TEM is conducted on dried samples that do not possess extended hydration spheres.³⁷ The micelles were stable in DI H₂O and in PBS buffer (pH = 7) over a period of 24 h (Figure S10). Their critical aggregation concentration measured via the Nile red assay was 10 μg/mL (Figure S13).

The kinetics of H₂S release were measured with the methylene blue assay.³⁸ By monitoring the absorbance over time, the relative rate of methylene blue formation can be measured and correlated to the rate of H₂S release.^{17,39} H₂S release could also be triggered by other biologically relevant thiols such as glutathione (GSH);¹⁷ however, GSH reduces methylene blue to the noncolored leucomethylene blue, making quantification of half-lives by the methylene blue assay difficult.⁴⁰ H₂S release kinetic experiments were carried out in the presence of Zn(OAc)₂ to capture the H₂S as it was released by the micelles. From these data, the pseudo-first-order half-life of H₂S release from the micelles triggered by Cys was calculated to be 3.3 ± 0.4 h (Figure 2). As expected, this half-life is significantly longer than that measured for a related small molecule SATO ($t_{1/2} = 22$ min). We attribute this difference in rate to the slow diffusion of the Cys trigger into the hydrophobic cores of the polymer micelles. The concentration profile of H₂S released from the micelles was also determined by conducting the methylene blue assay in the absence of the trapping agent Zn(OAc)₂. The concentration of H₂S at each time point was then calculated using a calibration curve. In this experiment, H₂S concentration reached a peaking value of ~9.5 μM after 1 h before slowly falling off (Figure S17). This low concentration of H₂S relative to H₂S donor is unsurprising

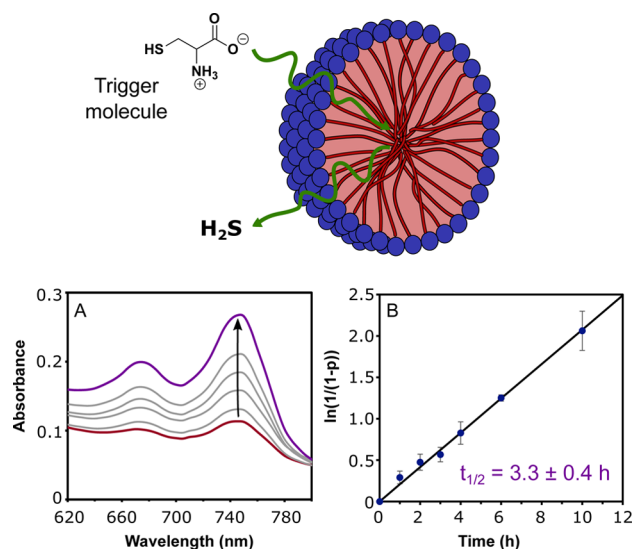


Figure 2. Kinetic analyses of H₂S release from micelles prepared from polymer **1**. (A) Raw output from methylene blue assay highlighting the increase in absorption at 750 nm. (B) Pseudo-first-order kinetic plot of H₂S release reaction. Reactions were conducted at [SATO] = 250 μM in the presence of 1 mM Cys and 2 mM Zn(OAc)₂ in phosphate buffer (pH = 7).

given the slow release rate of the micelles and the transient nature of H₂S.

We investigated the impact of the slow, sustained release of H₂S from SATO-functionalized micelles versus its burst release from Na₂S in cell viability by using a clonogenic assay. As a proof-of-concept, we selected two well-established and contrasting cellular models: HCT116 colon carcinoma cells, the model of choice for many cancer biology studies, and immortalized NIH/3T3 fibroblasts, a spontaneously generated cell line that retains major normal characteristics and is considered the “normal” standard for comparisons with transformed cells. These cell lines, besides being relatively easy to manipulate, have been shown to be, in the case of HCT116, invasive and motile *in vitro*,^{41,42} highly tumorigenic in xenograft experiments,⁴³ and metastatic in orthotopic models;⁴⁴ whereas NIH/3T3 fibroblasts retain major normal cell characteristics including contact inhibition and monolayer growth and are incapable of inducing tumorigenesis when injected into animals.⁴⁵

Experiments were performed by treating cells with micelles of polymer **1** in the presence or absence of Cys, Cys alone, and various other controls for 24 h, followed by quantification of the number of viable cells in each treatment group. A significant, concentration-dependent decrease in cell viability was observed for HCT116 cells treated with active micelles in the presence of added Cys (Figure 3A). H₂S released from micelles of polymer **1** led to a less pronounced, decrease in viability for NIH/3T3 cells. Other related studies show an increase in NIH/3T3 cell viability with added H₂S.^{39,46} The reason for the discrepancy between our studies here and previous reports is unclear, but it may be due to the rate of H₂S release or minor differences in how the experiments were conducted. No significant decrease in viability was observed for either cell line for micelles in the absence of Cys (which would not produce H₂S) or Cys alone (Figure 3B). Additionally, inactive micelles prepared from a precursor to polymer **1** that lacked SATO functionalization (and cannot produce H₂S) had

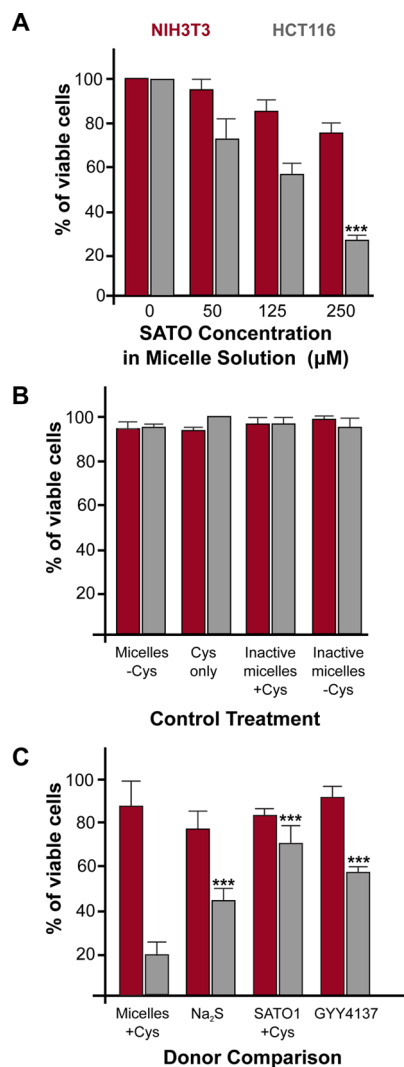


Figure 3. Clonogenic survival assay. (A) Titration of cells with active micelles prepared from polymer **1** in the presence of 1 mM Cys. Statistical significance was determined by paired *t* test; *** indicates $p < 0.001$ compared to cell media alone. (B) Control experiments demonstrating that toxicity toward cancer cells derives from H₂S release from the active micelles, which only occurs in the presence of Cys. Polymer concentration was held constant at 8.3 μM, and Cys was applied at 1 mM in all cases. (C) Comparison of the effect of active micelles to other common H₂S donors on cell viability. Donor concentration was 250 μM for all experiments (in terms of [SATO] for the micelles), and Cys was applied at 1 mM where noted. Statistical significance was determined by paired *t* test; *** indicates $p < 0.001$ compared to active micelles. In all experiments, clonogenic assays of NIH/3T3 and HCT116 cells (red and gray bars, respectively) were performed in 6-well plates after treatment for 24 h. Data are presented as the mean ± SD from 2–3 independent experiments performed in triplicate.

a similarly negligible effect on the viability of HCT116 or NIH/3T3 cells, both with and without added Cys. Finally, cells were treated with byproducts of the H₂S-releasing reaction, shown in Scheme S1, to determine their effect on cell viability. A solution of spent micelles was prepared by treating the micelles with 1 mM Cys in PBS buffer for 24 h. This spent micelle solution was assumed to contain both *N*-benzoylcysteine and cystine based on previous experiments with small molecule SATOs.¹⁷ The spent micelle solution exhibited no significant cytotoxicity

toward either cell line (Figure S15A). The cells were also treated with NH_4Cl , a source of NH_4^+ , which we hypothesize is formed as a byproduct of H_2S release. The applied NH_4Cl did not reduce cell viability in the concentration range tested (Figure S15B). Taken together, these control experiments suggest that the observed decrease in viability in HTC116 cells treated with active micelles originates from H_2S . Importantly, the difference in the survival of the two cell types indicates some selectivity for these micelles in killing cancer cells.

In addition, the reduction in cell viability observed with H_2S -releasing micelles of polymer **1** was compared to other common H_2S donors (Figure 3C), including Na_2S , SATO1 (a small molecule SATO ((C_6H_5) $\text{C}=\text{OSN}=\text{CH}(\text{C}_6\text{H}_4$)- COOH)), and GYY4137 (an H_2S donor with a release half-life on the order of days–weeks). In all cases, the H_2S -releasing micelles significantly decreased cell viability in HCT116 cells compared to alternative H_2S donors. No significant changes in viability were observed for NIH/3T3 cells across the different donor types. We attribute the enhanced toxicity of the micelles toward HCT116 cells compared to that of alternative donors to release rate. More mechanistic studies will be needed to optimize dosage and release rates and to identify any selective intermediary molecules involved.

CONCLUSIONS

In summary, we have prepared H_2S -releasing micelles based on SATO-functionalized polymer amphiphiles. The micelles significantly reduced the survival of HCT116 cells compared to other common H_2S donors, including Na_2S , a small molecule SATO, and GYY4137. Promisingly, the micelles were well tolerated by healthy NIH/3T3 cells. These H_2S -releasing micelles provide a valuable tool for studying H_2S in biological systems, both in vitro and as potential targeted H_2S delivery vehicles in vivo.

ASSOCIATED CONTENT

Supporting Information

The Supporting Information is available free of charge on the ACS Publications website at DOI: 10.1021/acs.molpharmaceut.6b01117.

Synthetic and experimental details, polymer and micelles characterization data, and additional H_2S release and cell toxicity data (PDF)

AUTHOR INFORMATION

Corresponding Author

*E-mail: jbmatson@vt.edu.

ORCID

Jeffrey C. Foster: 0000-0002-9097-8680

John B. Matson: 0000-0001-7984-5396

Notes

The authors declare no competing financial interest.

ACKNOWLEDGMENTS

This work was supported by the National Science Foundation (DMR-1454754 to J.B.M. and MCB-1517298 to C.V.F.) and the Virginia Tech Institute for Critical Technology and Applied Science (JFC12-256). We also thank 3M for support of this work through a Non-Tenured Faculty Award to J.B.M. We are grateful to Chris Winkler for assistance with TEM, Prof. Rick

Davis for use of the DLS instrument, and Xiangping Fu for her excellent technical support.

REFERENCES

- (1) Wang, R. Two's company, three's a crowd: can H_2S be the third endogenous gaseous transmitter? *FASEB J.* **2002**, *16* (13), 1792–1798.
- (2) Mustafa, A. K.; Gadalla, M. M.; Snyder, S. H. Signaling by Gasotransmitters. *Sci. Signaling* **2009**, *2* (68), re2.
- (3) Wang, R. Physiological Implications of Hydrogen Sulfide: A Whiff Exploration That Blossomed. *Physiol. Rev.* **2012**, *92* (2), 791–896.
- (4) Szabo, C. Hydrogen sulphide and its therapeutic potential. *Nat. Rev. Drug Discovery* **2007**, *6* (11), 917–935.
- (5) Papapetropoulos, A.; Pyriochou, A.; Altaany, Z.; Yang, G.; Marazioti, A.; Zhou, Z.; Jeschke, M. G.; Branski, L. K.; Herndon, D. N.; Wang, R.; Szabo, C. Hydrogen sulfide is an endogenous stimulator of angiogenesis. *Proc. Natl. Acad. Sci. U. S. A.* **2009**, *106* (51), 21972–21977.
- (6) Calvert, J. W.; Coetzee, W. A.; Lefer, D. J. Novel Insights Into Hydrogen Sulfide-Mediated Cytoprotection. *Antioxid. Redox Signaling* **2010**, *12* (10), 1203–1217.
- (7) Kashfi, K.; Olson, K. R. Biology and therapeutic potential of hydrogen sulfide and hydrogen sulfide-releasing chimeras. *Biochem. Pharmacol.* **2013**, *85* (5), 689–703.
- (8) Shibuya, N.; Koike, S.; Tanaka, M.; Ishigami-Yuasa, M.; Kimura, Y.; Ogasawara, Y.; Fukui, K.; Nagahara, N.; Kimura, H. A novel pathway for the production of hydrogen sulfide from D-cysteine in mammalian cells. *Nat. Commun.* **2013**, *4*, 1366.
- (9) Bailey, T. S.; Pluth, M. D. Chemiluminescent Detection of Enzymatically Produced Hydrogen Sulfide: Substrate Hydrogen Bonding Influences Selectivity for H_2S over Biological Thiols. *J. Am. Chem. Soc.* **2013**, *135* (44), 16697–16704.
- (10) Montoya, L. A.; Pluth, M. D. Selective turn-on fluorescent probes for imaging hydrogen sulfide in living cells. *Chem. Commun.* **2012**, *48* (39), 4767–4769.
- (11) Peng, B.; Zhang, C.; Marutani, E.; Pacheco, A.; Chen, W.; Ichinose, F.; Xian, M. Trapping Hydrogen Sulfide (H_2S) with Diselenides: The Application in the Design of Fluorescent Probes. *Org. Lett.* **2015**, *17* (6), 1541–1544.
- (12) Lin, V. S.; Chen, W.; Xian, M.; Chang, C. J. Chemical probes for molecular imaging and detection of hydrogen sulfide and reactive sulfur species in biological systems. *Chem. Soc. Rev.* **2015**, *44* (14), 4596–4618.
- (13) Zhang, H.; Kong, X.; Tang, Y.; Lin, W. Hydrogen Sulfide Triggered Charge-Reversal Micelles for Cancer-Targeted Drug Delivery and Imaging. *ACS Appl. Mater. Interfaces* **2016**, *8* (25), 16227–39.
- (14) Zhao, Y.; Wang, H.; Xian, M. Cysteine-activated hydrogen sulfide (H_2S) donors. *J. Am. Chem. Soc.* **2011**, *133*, 15–17.
- (15) Wallace, J. L. Hydrogen sulfide-releasing anti-inflammatory drugs. *Trends Pharmacol. Sci.* **2007**, *28* (10), 501–505.
- (16) Kodela, R.; Chattopadhyay, M.; Kashfi, K. NOSH-Aspirin: A Novel Nitric Oxide–Hydrogen Sulfide-Releasing Hybrid: A New Class of Anti-inflammatory Pharmaceuticals. *ACS Med. Chem. Lett.* **2012**, *3* (3), 257–262.
- (17) Foster, J. C.; Powell, C. R.; Radzinski, S. C.; Matson, J. B. S-Aroylthioximes: A Facile Route to Hydrogen Sulfide Releasing Compounds with Structure-Dependent Release Kinetics. *Org. Lett.* **2014**, *16* (6), 1558–1561.
- (18) Devarie-Baez, N. O.; Bagdon, P. E.; Peng, B.; Zhao, Y.; Park, C.-M.; Xian, M. Light-Induced Hydrogen Sulfide Release from “Caged” gem-Dithiols. *Org. Lett.* **2013**, *15* (11), 2786–2789.
- (19) Zhao, Y.; Biggs, T. D.; Xian, M. Hydrogen sulfide (H_2S) releasing agents: chemistry and biological applications. *Chem. Commun.* **2014**, *50* (80), 11788–11805.
- (20) Chattopadhyay, M.; Kodela, R.; Nath, N.; Dastagirzada, Y. M.; Velazquez-Martinez, C. A.; Boring, D.; Kashfi, K. Hydrogen sulfide-releasing NSAIDs inhibit the growth of human cancer cells: A general

property and evidence of a tissue type-independent effect. *Biochem. Pharmacol.* **2012**, *83* (6), 715–722.

(21) Li, L.; Whiteman, M.; Guan, Y. Y.; Neo, K. L.; Cheng, Y.; Lee, S. W.; Zhao, Y.; Baskar, R.; Tan, C.-H.; Moore, P. K. Characterization of a Novel, Water-Soluble Hydrogen Sulfide-Releasing Molecule (GYY4137). *Circulation* **2008**, *117* (18), 2351–2360.

(22) Szczesny, B.; Módis, K.; Yanagi, K.; Coletta, C.; Le Trionnaire, S.; Perry, A.; Wood, M. E.; Whiteman, M.; Szabo, C. AP39, a novel mitochondria-targeted hydrogen sulfide donor, stimulates cellular bioenergetics, exerts cytoprotective effects and protects against the loss of mitochondrial DNA integrity in oxidatively stressed endothelial cells in vitro. *Nitric Oxide* **2014**, *41*, 120–130.

(23) Wu, D.; Si, W.; Wang, M.; Lv, S.; Ji, A.; Li, Y. Hydrogen sulfide in cancer: Friend or foe? *Nitric Oxide* **2015**, *50*, 38–45.

(24) Lee, Z. W.; Teo, X. Y.; Tay, E. Y. W.; Tan, C. H.; Hagen, T.; Moore, P. K.; Deng, L. W. Utilizing hydrogen sulfide as a novel anti-cancer agent by targeting cancer glycolysis and pH imbalance. *Br. J. Pharmacol.* **2014**, *171* (18), 4322–4336.

(25) Filomeni, G.; Aquilano, K.; Rotilio, G.; Ciriolo, M. R. Reactive Oxygen Species-dependent c-Jun NH2-terminal Kinase/c-Jun Signaling Cascade Mediates Neuroblastoma Cell Death Induced by Diallyl Disulfide. *Cancer Res.* **2003**, *63* (18), 5940–5949.

(26) Cairns, R.; Papandreou, I.; Denko, N. Overcoming Physiologic Barriers to Cancer Treatment by Molecularly Targeting the Tumor Microenvironment. *Mol. Cancer Res.* **2006**, *4* (2), 61–70.

(27) Szabo, C.; Coletta, C.; Chao, C.; Módis, K.; Szczesny, B.; Papapetropoulos, A.; Hellmich, M. R. Tumor-derived hydrogen sulfide, produced by cystathionine- β -synthase, stimulates bioenergetics, cell proliferation, and angiogenesis in colon cancer. *Proc. Natl. Acad. Sci. U. S. A.* **2013**, *110* (30), 12474–12479.

(28) *Chemistry, Biochemistry and Pharmacology of Hydrogen Sulfide*; Springer International Publishing: Switzerland, 2015; Vol. 230.

(29) Foster, J. C.; Matson, J. B. Functionalization of Methacrylate Polymers with Thiooximes: A Robust Postpolymerization Modification Reaction and a Method for the Preparation of H₂S-Releasing Polymers. *Macromolecules* **2014**, *47* (15), 5089–5095.

(30) Hasegawa, U.; van der Vlies, A. J. Design and Synthesis of Polymeric Hydrogen Sulfide Donors. *Bioconjugate Chem.* **2014**, *25* (7), 1290–1300.

(31) Carter, J. M.; Qian, Y.; Foster, J. C.; Matson, J. B. Peptide-based hydrogen sulphide-releasing gels. *Chem. Commun. (Cambridge, U. K.)* **2015**, *51* (66), 13131–13134.

(32) Long, T. R.; Wongrakpanich, A.; Do, A.-V.; Salem, A. K.; Bowden, N. B. Long-term release of a thiobenzamide from a backbone functionalized poly(lactic acid). *Polym. Chem.* **2015**, *6* (40), 7188–7195.

(33) Qian, Y.; Matson, J. B. Gasotransmitter delivery via self-assembling peptides: Treating diseases with natural signaling gases. *Adv. Drug Delivery Rev.* **2016**, DOI: 10.1016/j.addr.2016.06.017.

(34) Nguyen, M. M.; Carlini, A. S.; Chien, M.-P.; Sonnenberg, S.; Luo, C.; Braden, R. L.; Osborn, K. G.; Li, Y.; Gianneschi, N. C.; Christman, K. L. Enzyme-Responsive Nanoparticles for Targeted Accumulation and Prolonged Retention in Heart Tissue after Myocardial Infarction. *Adv. Mater.* **2015**, *27* (37), 5547–5552.

(35) Ambade, A. V.; Savariar, E. N.; Thayumanavan, S. Dendrimeric Micelles for Controlled Drug Release and Targeted Delivery. *Mol. Pharmaceutics* **2005**, *2* (4), 264–272.

(36) Willcock, H.; O'Reilly, R. K. End group removal and modification of RAFT polymers. *Polym. Chem.* **2010**, *1* (2), 149–157.

(37) Matson, J. B.; Grubbs, R. H. Synthesis of Fluorine-18 Functionalized Nanoparticles for use as in vivo Molecular Imaging Agents. *J. Am. Chem. Soc.* **2008**, *130* (21), 6731–6733.

(38) Siegel, L. M. A direct microdetermination for sulfide. *Anal. Biochem.* **1965**, *11* (1), 126–132.

(39) Feng, S.; Zhao, Y.; Xian, M.; Wang, Q. Biological thiols-triggered hydrogen sulfide releasing microfibers for tissue engineering applications. *Acta Biomater.* **2015**, *27*, 205–213.

(40) Kelner, M. J.; Alexander, N. M. Methylene blue directly oxidizes glutathione without the intermediate formation of hydrogen peroxide. *J. Bio. Chem.* **1985**, *260* (28), 15168–15171.

(41) Sawhney, R. S.; Zhou, G.-H. K.; Humphrey, L. E.; Ghosh, P.; Kreisberg, J. I.; Brattain, M. G. Differences in Sensitivity of Biological Functions Mediated by Epidermal Growth Factor Receptor Activation with Respect to Endogenous and Exogenous Ligands. *J. Biol. Chem.* **2002**, *277* (1), 75–86.

(42) Awwad, R. A.; Sergina, N.; Yang, H.; Ziober, B.; Willson, J. K. V.; Zborowska, E.; Humphrey, L. E.; Fan, R.; Ko, T. C.; Brattain, M. G.; Howell, G. M. The Role of Transforming Growth Factor α in Determining Growth Factor Independence. *Cancer Res.* **2003**, *63* (15), 4731–4738.

(43) Wang, J.; Sun, L.; Myeroff, L.; Wang, X.; Gentry, L. E.; Yang, J.; Liang, J.; Zborowska, E.; Markowitz, S.; Willson, J. K. V.; Brattain, M. G. Demonstration That Mutation of the Type II Transforming Growth Factor β Receptor Inactivates Its Tumor Suppressor Activity in Replication Error-positive Colon Carcinoma Cells. *J. Biol. Chem.* **1995**, *270* (37), 22044–22049.

(44) Rajput, A.; Dominguez San Martin, I.; Rose, R.; Beko, A.; LeVea, C.; Sharratt, E.; Mazurchuk, R.; Hoffman, R. M.; Brattain, M. G.; Wang, J. Characterization of HCT116 Human Colon Cancer Cells in an Orthotopic Model. *J. Surg. Res.* **2008**, *147* (2), 276–281.

(45) Todaro, G. J.; Green, H. Quantitative studies of the growth of mouse embryo cells in culture and their development into established lines. *J. Cell Biol.* **1963**, *17* (2), 299–313.

(46) Wu, J.; Li, Y.; He, C.; Kang, J.; Ye, J.; Xiao, Z.; Zhu, J.; Chen, A.; Feng, S.; Li, X.; Xiao, J.; Xian, M.; Wang, Q. Novel H₂S Releasing Nanofibrous Coating for In Vivo Dermal Wound Regeneration. *ACS Appl. Mater. Interfaces* **2016**, *8* (41), 27474–27481.